

Original Research

Model for Concomitant Microdialysis Sampling of the Pons and Cerebral Cortex in Rhesus Macaques (*Macaca mulatta*)

Cynthia M McCully,^{1*} Devang Pastakia,¹ John Bacher,² Marvin L Thomas 3rd,² Emilie A Steffen-Smith,¹ Kadharbatha Saleem,³ Robert F Murphy,¹ Stuart Walbridge,⁴ Lauren Brinster,² Brigitte C Widemann,¹ and Katherine E Warren¹

Pediatric diffuse intrinsic pontine gliomas are aggressive brainstem tumors that fail to respond to treatment. We hypothesize that the protective features of the pons may hinder chemotherapeutic agents from entering pontine tissue compared with cortical brain tissue. To test this hypothesis, we developed a unique nonhuman primate model using microdialysis, a continuous in vivo extracellular sampling technique, to compare drug exposure concurrently in pontine tissue, cortical tissue, CSF, and plasma after intravenous administration of chemotherapeutic agents. The surgical coordinates and approach for microdialysis cannula–probe placement were determined in 5 adult male rhesus monkeys (*Macaca mulatta*) by using MRI. Microdialysis cannulas–probes were implanted stereotactically in the brain, retrodialysis was performed to measure relative recovery, and a 1-h intravenous infusion of temozolomide was administered. Continuous microdialysis samples were collected from the pons and cortex over 4 h with concurrent serial plasma and CSF samples. Postsurgical verification of microdialysis cannula–probe placement was obtained via MRI in 3 macaques and by gross pathology in all 5 animals. The MRI-determined coordinates and surgical methodologies resulted in accurate microdialysis probe placement in the pons and cortex in 4 of the 5 macaques. Histologic examination from these 4 animals revealed negligible tissue damage to the pontine and cortical tissue from microdialysis. One macaque was maintained for 8 wk and had no deficits attributed to the procedure. This animal model allows for the determination of differences in CNS penetration of chemotherapeutic agents in the pons, cortex, and CSF after systemic drug administration.

Abbreviations: DIPG, diffuse intrinsic pontine glioma; ECF, extracellular fluid.

Pediatric diffuse intrinsic pontine gliomas (DIPG) are aggressive tumors that cannot be surgically resected due to their location, and are resistant to chemotherapeutic and radiation therapies. As a result, children with DIPG have a dismal prognosis with median survival less than one year from diagnosis. One hypothesis for the poor efficacy of treatment is that innate CNS protective features, such as the blood–brain barrier and the blood–CSF barrier, shield the brainstem to a higher degree given its critical functions, and isolate pontine gliomas from treatment. To test this hypothesis, we developed a nonhuman primate model in rhesus monkeys to evaluate pontine tissue pharmacokinetics by using microdialysis, a continuous in vivo extracellular sampling technique based on diffusion. Microdialysis is the ‘gold standard’ for in vivo sampling methodologies in the CNS, enabling the collection of extracellular tissue fluid via passive diffusion by using a semipermeable membrane probe.

A nonhuman primate model demonstrating the feasibility of microdialysis sampling from cortical brain tissue with concurrent pharmacokinetic sampling during chemotherapeutic drug

administration has previously been established,^{3–5,7} but there are no current animal models that measure drug penetration into the pons. The location of the pons deep within the brain, as well as the vital brainstem functions associated with the pons, present additional obstacles to accurate microdialysis probe placement and sample collection. The objectives of the current study were to develop imaging and surgical procedures for the accurate placement of a microdialysis probe within the pons of rhesus monkeys for sample collection, to establish a method to perform microdialysis simultaneously in multiple CNS regions, and to develop a mechanism to perform repeated microdialysis in the same areas with a single invasive surgical procedure. This model allows for the pharmacokinetic comparison of drug penetration into pontine tissue, in conjunction with cortical tissue, plasma, and CSF, after intravenous administration.

Materials and Methods

The National Cancer Institute IACUC approved this study.

Five adult male rhesus monkeys (*Macaca mulatta*; age, 10 to 15 y; weight, 9.7 to 14.4 kg) negative for SRV, SIV, and herpes B virus were used. The animals were socially housed in groups, fed LabDiet Monkey Chow no. 5038 (PMI, St Louis, MO) with water ad libitum, and cared for in accordance with the *Guide for the Care and Use of Laboratory Animals*.⁶

Received: 04 Oct 2012. Revision requested: 31 Oct 2012. Accepted: 04 Feb 2013.

¹National Cancer Institute, ²Office of Research Services, ³National Institute of Mental Health, and ⁴National Institute of Neurologic Diseases and Stroke, Bethesda, Maryland.

*Corresponding author. Email: mccullyc@mail.nih.gov

Determination of surgical coordinates. Prior to the surgical procedure, the macaques underwent MRI to determine the length necessary for the custom pontine microdialysis cannula and to establish surgical coordinates for the pons and cortex. Three macaques were used to determine the cannula length; individual cortical and pontine coordinates were determined in all 5 animals. Each macaque was anesthetized with ketamine (10 mg/kg IM) and dexmedetomidine (1000 µg/m²), maintained with isoflurane (1% to 2%) and oxygen (2 L/min), and placed in a custom MRI-compatible stereotactic unit (model 1530M, David Kopf Instruments, Tujunga, CA). Vitamin E was used in 2 locations as a marker during scanning. A capsule was taped temporarily to the left side of the head as an external fiducial marker for the stereotactic zero point and was removed after scanning. In addition, the ear bars were filled with vitamin E liquid as a reference fluid marker to enable visualization of stereotactic zero. All scans were acquired on a 3-T MRI scanner (Philips Healthcare, Best, Netherlands) and included 3D T1-weighted images (field of view, 110 mm; repetition time, 25 ms; echo time, 4.3 ms; matrix, 256 × 256; slice thickness, 1 mm).

OsiriX imaging software (version 3.9.4, Antoine Rosset, Bernex, Geneva)¹⁰ was used to determine the length of the microdialysis cannula and calculate the coordinates of the pons on the presurgical scans. The surgical approach, pontine coordinates, and length of the microdialysis cannula and probe were determined so that the ventricles and major blood vessels could be avoided.¹¹ The 5 measurements comprising the coordinates were: the angle from the midline, the distance from the midline, the distance and direction from the ear bars, and the depth from the ear bars. To determine the angle of approach to the pons (that is, the angle from the midline), a line equal in length to the sum of the cannula and probe lengths was drawn from the skull to the pons, avoiding the ventricles and major blood vessels (Figure 1 B). The angle was determined by the difference (in degrees) from the midline to the microdialysis cannula–probe line. Sagittal views were used for confirmation. The distance from the midline was defined as the distance the microdialysis cannula–probe line extended past the intersection with the midline (Figure 1 B). The distance and direction were determined by the difference in slice number from that in which the ear bars (that is, stereotactic zero) first were visible (Figure 1 A) to the slice number used for calculating the pontine measurements (Figure 1 B) given the thickness per slice and direction of the scan. For example, slice 41 was chosen for the pontine calculations when the ear bars were visualized in slice 31. By using a 1-mm slice thickness and slices numbered from posterior to anterior, the direction was anterior with a distance of 10 mm. The depth was determined by the difference between the Y coordinate value (in mm) at the ear bars (Figure 1 A) with that of the Y coordinate value (in mm) at the distal end of the microdialysis cannula–probe (Figure 1 B).

Surgical procedure. Fasted macaques were anesthetized with ketamine (10 mg/kg IM), glycopyrolate (0.01 mg/kg IM), and propofol (10 mg/kg IV) and intubated. Anesthesia was maintained via isoflurane (1% to 2%) and oxygen at a total flow rate of 2 L/min. Temperature, heart rate, pO₂, electrocardiographic response, and end-tidal pCO₂ were monitored continuously. The macaques were positioned in ventral recumbency, with the head centered and secured in a standard stereotactic unit (model 1504, David Kopf Instruments). Surgery was performed by using aseptic technique, and microdialysis cannulas and probes were sterilized

with ethylene oxide. A 10- to 12-cm midline skin incision was made over the frontal and parietal bones, exposing the underlying skull. The periosteum was incised and retracted laterally with the temporalis muscle. A left surgical approach was chosen, and a 20 mm × 20 mm opening was created in the skull at the stereotactically determined entry point. The underlying dura mater was opened. Both microdialysis cannulas were positioned by using stereotactic carriers. The pons microdialysis cannula and probe were positioned by using the coordinates determined through MRI for each macaque, with the pontine cannula positioned slightly superior to the pons. The cortical microdialysis cannula was positioned by using the coordinates determined through MRI for each macaque, 15 to 20 mm anterior to the microdialysis pontine cannula and 5 to 7 mm off midline. The stylets for the pontine and cortical microdialysis cannulas were removed, and the probes were lowered into the respective tissues via the cannulas. The microdialysis probe inlet–outlet capillaries were connected to a microdialysis infusion pump (model 106, CMA, Solna, Sweden) operating at a flow rate of 0.3 µL/min.

Microdialysis procedure. Custom microdialysis cannulas and probes (model 11, CMA) were used in both the cortex and pons (Figure 2). Both cannulas had an outer dimension of 0.38 mm. Probes consisted of a shaft equal in length to the cannula and a cuprophane membrane with an outer diameter of 0.24 mm and a 6000-Dalton molecular-weight cutoff for diffusion.

Retrodialysis was done to determine the *in vivo* recovery for each microdialysis probe.^{2,13} Because this corrective measurement is compound-dependent, temolozomide was perfused through each microdialysis probe. The resulting dialysate sample was collected for calibration of each probe. At the completion of retrodialysis, the perfusate was changed to CNS perfusion fluid (CMA) and flushed twice to clear the probe of drug. After retrodialysis, temolozomide (10 mg/kg) was infused intravenously into the cephalic vein over 1 h.

Sample collection. Single continuous microdialysis sampling began at the start of the temolozomide infusion from both the cortical and pontine tissues. Serial plasma samples were collected from a saphenous vein via a percutaneous catheter. CSF was collected concurrently via a subarachnoid catheter¹ that was placed contralateral to the microdialysis cannulas and probes. A 10-mm opening in the skull was created adjacent to the lateral midline, exposing the superior sagittal sinus. An avascular area of the dura, lateral to the sinus, was opened, and a silastic catheter (inner diameter, 0.025 in.; outer diameter, 0.047 in.; Dow Corning, Midland, MI) prefilled with normal saline was passed into the subarachnoid space. CSF was obtained by gravitational flow.

Validation of microdialysis cannula and probe placement. At the conclusion of sample collection, the pontine and cortical cannulas were secured to the skulls of all macaques by using screws and Cerebond adhesive (Plastics One, Roanoke, VA). In the one animal, which was followed for 8 wk, the microdialysis probes were removed and replaced with the stylet prior to closure of the incision site. The macaques then were removed from the stereotactic unit. MRI was performed in 3 of the 5 macaques to verify cannula–probe placement after surgery. For these animals, anesthesia was maintained by using ketamine (10 mg/kg IM), dexmedetomidine (1000 µg/m²), and isoflurane (1% to 2%) and oxygen (2 L/min); heart rate, oxygen saturation, electrocardiographic response, and end-tidal CO₂ were monitored continuously throughout the scanning procedure. All 5 macaques were euthanized (pentobarbital,

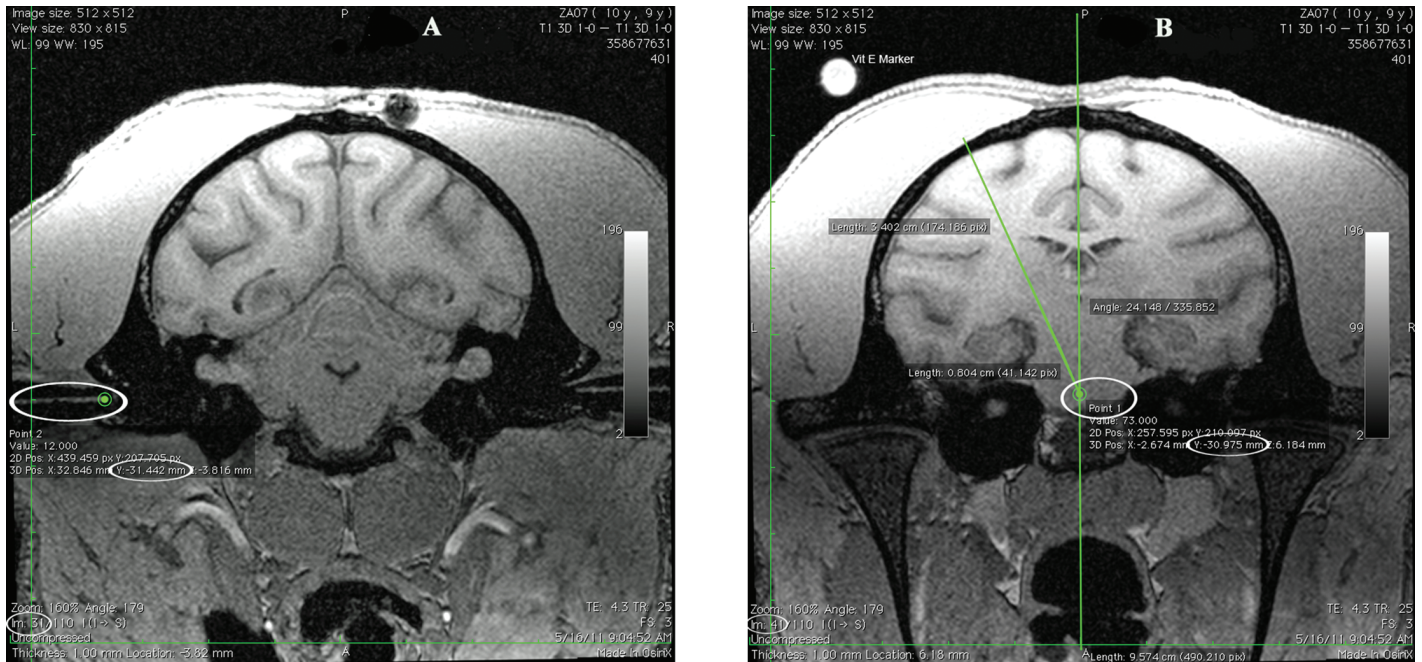


Figure 1. Presurgical MRI scans developing coordinates in animal ZA07. (A) Coronal precontrast T1-weighted presurgical MRI showing the ear bars at stereotactic zero in image 31. Each image is 1 mm in thickness. Ear bars are filled with vitamin E. (B) Presurgical pontine measurements with a 24° angle and 0 mm off midline. Distance and direction from the zero point is anterior 10 mm. Depth is 0.5 mm.

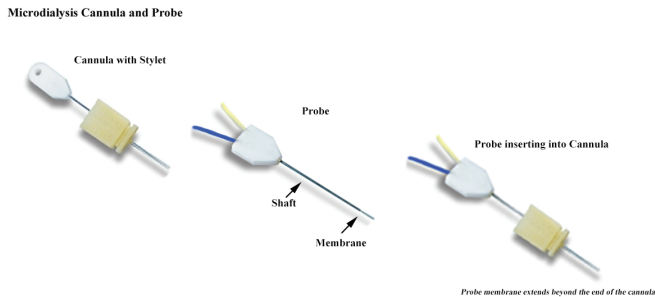


Figure 2. Microdialysis cannula and probe.

80 mg/kg IV, and Beuthanasia-D, 1 mL/4 kg IV; Merck Animal Health, Summit, NJ), 4 of which were euthanized postprocedurally without regaining consciousness (as part of the experimental design) and without procedural complications. In addition, 2 of the 4 macaques that did not regain consciousness were euthanized at the conclusion of the postsurgical MRI; the remaining 2 were euthanized at the conclusion of sample collection, because postsurgical MRI was unavailable. The remaining macaque was followed for 8 wk prior to euthanasia and was scanned immediately and at 1 and 8 wk after surgery. In all 5 macaques, placement of the microdialysis cannula and probe was verified via gross pathology. Effects on tissue were determined by histopathology.

Recurrent microdialysis sampling. The macaque that was maintained underwent a repeat temolozomide microdialysis study at 8 wk. The animal was fasted, anesthetized, monitored, and positioned as previously described. Surgery was performed by using aseptic technique. A 6- to 8-cm skin incision was made over the existing microdialysis cannulas, the cannula stylets were removed, and the microdialysis cortical and pontine probes were

introduced via the existing microdialysis cannulas. Sample collection and temolozomide administration occurred as previously described.

Sample analysis. Temolozomide concentration was analyzed by using a previously described method.⁸ Normal monkey plasma was used for plasma standards, which ranged in concentration from 0.05 to 1.0 μ M. CNS perfusion fluid was used for microdialysis standards, which ranged in concentration from 1.0 to 50 nM.

In vivo recovery of both probes was accomplished by using retrodialysis, a calibration procedure in which a known concentration of the study agent is infused into the target tissue and the resulting sample is used to determine the degree of recovery of the study agent in the target tissue. Temolozomide was infused into both the cortical and pontine probes at 2.5, 10, or 25 ng/mL at 0.3 μ L/min for an average of 2 h. In vivo recovery¹² was calculated as relative loss from the following equation:

$$\text{Recovery} = [\text{Perfusate}] - [\text{Dialysate}] \div [\text{Perfusate}] \times 100\%,$$

where [Perfusate] is the known concentration of the solution infused and [Dialysate] is the drug concentration of the sample from the tissue. The extracellular fluid concentrations (ECF) for temolozomide in both the cortex and pons were calculated by dividing the measured temolozomide dialysate concentration by the in vivo probe recovery. The ECF cortex and pons levels represent an average concentration of temolozomide over the sampling interval; therefore the ECF AUC_{0 to 3h} for the cortex and pons were calculated by multiplying the ECF temolozomide concentrations by the collection interval.⁷ The plasma and CSF temolozomide AUC_{0 to 3h} were calculated by using the linear trapezoidal method $\text{AUC} = [T_n - T_{n-1}] \times [C_{n-1} + C_n] \div 2$.

Table 1. Pontine coordinates

Animal no.	Angle (degrees)	Distance of distal tip off midline (mm)	Direction from earbars	Distance from earbars (mm)	Depth from earbars (mm)	Successful?
ZA07	24	0	Anterior	10	0.5	Yes
RQ2987	35	1.0	Anterior	24	10	No
V29	39	1.0	Anterior	10	2.0	Yes
T84	25	2.5	Anterior	10	4.5	Yes
R37	12	2.0	Anterior	7	3.0	Yes

Results

Validation of microdialysis cannula length and surgical coordinates. For the nonsurvival macaques, microdialysis cannula lengths, which were predetermined by using the preoperative scans of 3 animals, were 34 mm (30 mm functional length without hub and stylet) and 10 mm (6 mm functional length without hub and stylet) for the pons and cortex, respectively. The membranes of the probes for the pons and cortex extended 8 mm beyond the cannula and into the tissue for microdialysis sampling to occur (Figure 2). The total lengths of the microdialysis cannula and probe were therefore 42 mm and 18 mm for the pons and cortex, respectively. For the macaque that was maintained for 8 wk after surgery, microdialysis cannula lengths, which were predetermined by using the preoperative scans of 2 animals, were 41 mm (37 mm functional length without hub and stylet) and 8 mm (4 mm functional length without hub and stylet) for the pons and cortex, respectively. The membranes of the probes for the pons and cortex extended 8 mm beyond the cannula and into the tissue for microdialysis sampling to occur (Figure 2). The total lengths of the microdialysis cannula and probe were therefore 49 mm and 12 mm for the pons and cortex, respectively. In 4 of the 5 macaque, the MRI-determined coordinates were accurate (Table 1).

Surgical procedure. Monitoring of heart and respiratory rates, end-tidal CO₂, and pO₂ remained normal in all macaques during surgical placement of the cannula and probe, sample collection, and imaging (for the animals that underwent postsurgical MRI). Because the maintenance of normal vital signs in anesthetized macaques that underwent the described surgical procedure, sampling, and scanning indicated success of a survival model, we allowed 1 macaque to recover after surgical implantation of microdialysis cortical and pons cannulas and maintained this animal for 8 wk after surgery. There was no evidence of neurologic sequelae attributed to the procedure.

Validation of microdialysis probe placement. The placement of the microdialysis cannula and probe was verified postsurgically in 4 of 5 animals. Scans of subject ZA07 (Figure 3) illustrate the correct placement of the microdialysis cannula and probe for both the pons and cortex. For the survival animal, macaque R37, scans obtained at 1 and 8 wk after surgery were coregistered to the immediate postoperative scan and demonstrated that the cannulas did not migrate (Figure 4).

Gross pathology was obtained for all 5 macaques. Correct placement of the microdialysis cannula and probe was verified for the cortex in all 5 animals and for the pons in 4 of the 5 animals. In the second study macaque, the pontine cannula and probe appeared to be anterior and deep to the target. This inaccuracy was attributed to elevation of the head relative to an oblique plane by the mouthpiece despite correct placement in the ear bars during the use of the MRI-compatible stereotactic unit. The loss of a parallel plane resulted in inaccurate coordinates.

Histopathology was obtained for the 4 macaques with correct placement of the microdialysis probe within both the cortex and pons. Small areas of hemorrhage in the neural tissue at the distal end of the microdialysis cannula, positioned slightly superior to the pons, were present, but tissue damage due to placement of the probe membrane in cortical or pontine tissue was negligible as evidenced by the absence of hemorrhage, edema, and lymphocytic infiltration (Figure 5).

Recurrent sampling. The reintroduction of the microdialysis cortical and pontine probes via existing microdialysis cannulas and subsequent sample collection was successful in the macaque that was maintained. This animal was euthanized for humane concerns due to advanced arthritis-associated lordosis that affected ambulation; this event was deemed unrelated to the initial surgical or sampling procedure.

Sample collection and analysis. Samples of plasma, CSF, and microdialysate were obtained from all 5 macaques. Sample analysis for temolozomide was performed in the 4 studies in which the pontine target was validated. A validating example of microdialysis probe recovery and temolozomide ECF and AUC_{0 to 3 h} for cortical and pontine tissue in the 8-wk survival animal is represented in Table 2.

Discussion

We have created and validated a unique nonhuman primate model that allows extracellular tissue sampling of the pons and cerebral cortex via microdialysis, with concurrent sampling of CSF and plasma, after intravenous drug administration. The results show that the method used to determine the coordinates and surgical approach for placement of the microdialysis cannula and probe for the pons was successful and the procedure feasible.

The success of the cannula and probe placement is dependent on the positioning of the macaque in a parallel plane during the presurgical MRI scan. All of the measurement for the coordinates are established relative to the ear bars at stereotactic zero. With the macaque properly placed in the ear bars, care must be taken to position the macaque vertically level with the mouthpiece, as the position of the mouthpiece can elevate the head to an oblique plane. Leveling the macaque in the horizontal plan is a rapid check, prior to scanning, to verify that the ear bars are being used correctly. Leveling of the animal in both planes eliminates inaccurate distance and depth measurements and allows for the use of 2 functionally different stereotactic units: one portable and compatible with MRI and the other that is fixed and stable for surgery.

The current study demonstrated that the macaques acutely tolerated microdialysis cannula and probe placement, as evidenced by stable vital signs during anesthesia. In addition, the macaque that was maintained for 8 wk after surgery had no demonstrable

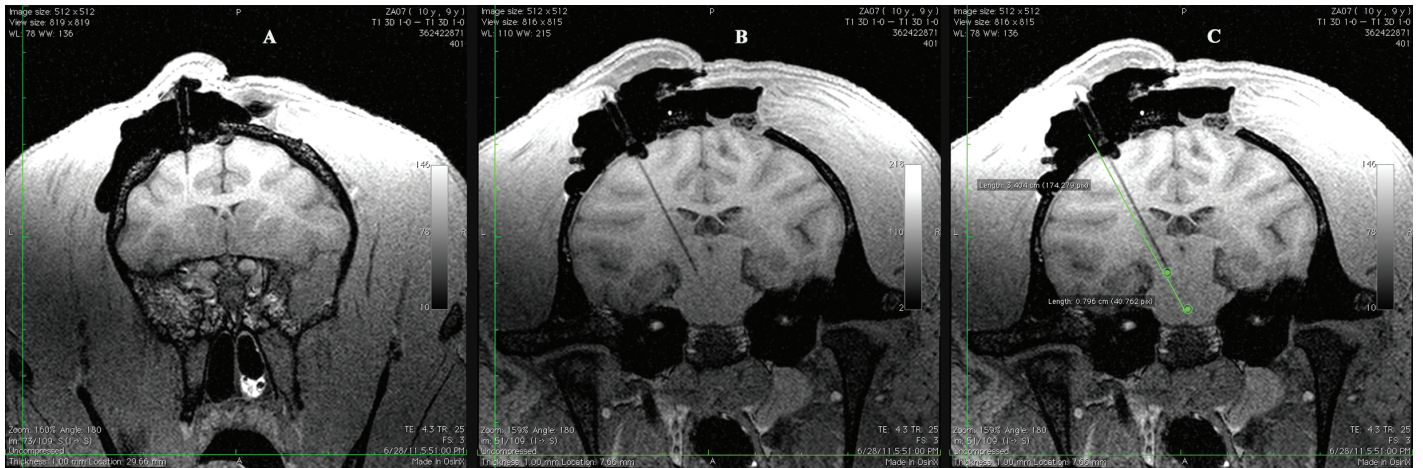


Figure 3. Postsurgical MRI scans validating placement of microdialysis cannula and probe in animal ZA07. (A) Cortical cannula visible with a faint outline of probe. (B) Pontine cannula visible with a faint outline of probe. (C) Pontine cannula and probe with measurements.



Figure 4. Postsurgical MRI scans validating placement and stability of the microdialysis pontine cannula in animal R37. (A) Immediately postoperatively. (B) 6 d postoperatively and coregistered to 9/18/12 scan. (C) 8 wk postoperatively and coregistered to 9/23/12 scan.

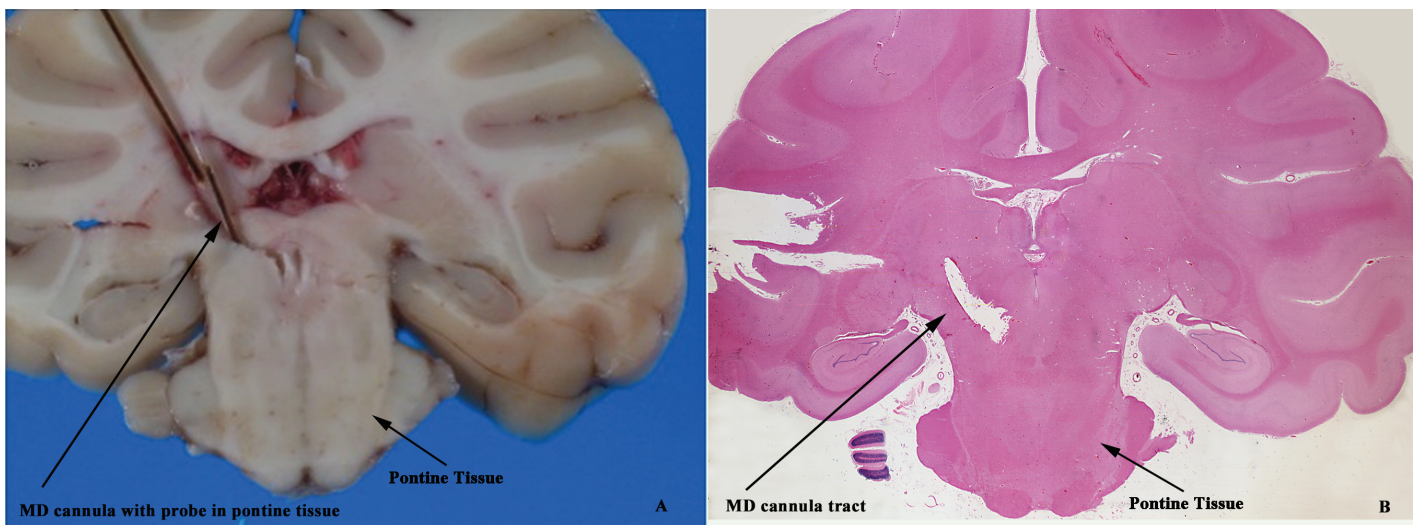


Figure 5. (A) Gross pathology and (B) histology for animal ZA07. (A) The microdialysis cannula was damaged at necropsy, but the path of the microdialysis cannula and probe in the pontine tissue are visible. (B) The tract of the microdialysis cannula is present, but there is negligible damage of pontine tissue. Hematoxylin and eosin stain; magnification, 4 \times .

Table 2. Cortical and pontine recoveries, concentration of temozolomide in extracellular fluid (TMZ ECF), and AUC in animal R37

	% Recovery	TMZ ECF (μM)	TMZ ECF AUC _{0-3h} ($\mu\text{M} \times \text{h}$)
Cortex	33.46 (66.54)	18.42	55.27
Pons	83.9 (16.1)	4.88	14.65

In vivo recovery is reported as relative loss, with relative recovery in parentheses.

neurologic complications from implantation or sampling. Furthermore, histopathology showed negligible pontine tissue damage after probe placement.

The pharmacokinetics and CNS penetration of temozolomide are well documented in humans⁸ and nonhuman primates,⁹ with a reported CSF to plasma AUC ratio of 0.33 and a half-life of 1.8 h. The CSF:plasma AUC ratio for the macaque that was maintained for 8 wk (R37) is 0.47; both the mean ECF and AUC of temozolomide were lower for pontine than cortical tissue with a pontine:cortical AUC ratio of 0.26. Although the model indicate geographic variability in temozolomide tissue concentrations, the number of animals tested was small and the procedure complex, with surgery, sampling, and scanning performed sequentially in a single day, limiting extended sampling times beyond steady state. Although the model was validated, as the sample analysis from macaque R37 (Table 2) demonstrates, additional testing and pharmacokinetic analysis of temozolomide and other chemotherapeutic agents using cortical and pontine microdialysis need to be performed before conclusions can be drawn regarding the geographic variability of CNS penetration of individual agents.

The uniqueness of this animal model lies not only within the ability to accurately access pontine pharmacokinetics in rhesus macaques but also in the opportunity to obtain microdialysis samples from pontine and cortical tissue concurrently for pharmacokinetic comparison. Determining any geographic variability in the penetration of chemotherapeutic drugs within the CNS is key to investigating the lack of efficacy of agents for brainstem tumors such as DIPG. No progress has been made in improving the outcome of children with DIPG in more than 3 decades, despite numerous clinical investigations of various chemotherapeutic agents. Rather than continuing to empirically treat these tumors with different agents, determining why chemotherapy fails globally in these tumors is crucial to improving the outcome of these patients. If limited CNS penetration of agents into the pons is verified, more suitable drug delivery techniques such as convection-enhanced delivery can be used as alternatives to systemic delivery.

Our nonhuman primate model is ideally suited to determine whether the lack of response by pediatric diffuse intrinsic pontine gliomas to treatment is associated with a lack of drug penetration into pontine tissue compared with cortical tissue. We will continue exploring this model by including additional survival animals that have a subcutaneous, semipermanent, closed system

for CNS microdialysis probe placement and continuous sampling and plan to evaluate additional chemotherapeutic agents.

Acknowledgments

We thank the National Cancer Institute, Laboratory Animal Science Program, Nonhuman Primate Staff, for their support and excellent animal care. Also, thank you to Renee Hill and Joelle Sarlls, National Institutes of Neurologic Disorders and Stroke, for their expertise and support.

References

1. **Bacher JD, Balis FM, McCully CL, Godwin KS.** 1994. Cerebral subarachnoid sampling of cerebrospinal fluid in the rhesus monkey. *Lab Anim Sci* **44**:148–152.
2. **Bungay PM, Dedrick RL, Fox E, Balis FM.** 2001. Probe calibration in transient microdialysis in vivo. *Pharm Res* **18**:361–366.
3. **Fox E, Bacher J, McCully CL, Bungay PM, Dedrick RL, Balis FM.** 2002. Zidovudine concentration in brain extracellular fluid measured by microdialysis: steady-state and transient results in the rhesus monkey. *J Pharmacol Exp Ther* **301**:1003–1011.
4. **Fox E, McCully CL, Bacher J, Bungay PM, Dedrick RL, Balis FM.** 2000. Comparison of in vitro and in vivo microdialysis calibration for tissue zidovudine concentrations in nonhuman primates. *Proc Am Assoc Cancer Res* **41**:721.
5. **Fox E, McCully CL, Bacher J, Bungay PM, Dedrick RL, Balis FM.** 2001. Brain, muscle, and blood pharmacokinetics of zidovudine in nonhuman primates using microdialysis. *Proc Am Assoc Cancer Res* **42**:83.
6. **Institute for Laboratory Animal Research.** 2011. Guide for the care and use of laboratory animals, 8th ed. Washington (DC): National Academies Press
7. **Jacobs S, McCully CL, Bacher J, Balis F, Fox E.** 2006. Extracellular fluid concentrations of platinum analogs in brain, blood, and muscle using microdialysis in a nonhuman primate model [abstract]. *Proc Am Assoc Cancer Res* **47**:1349.
8. **Meany HJ, Warren KE, Fox E, Cole DE, Aikin AA, Balis FM.** 2009. Pharmacokinetics of temozolomide administered in combination with O6-benzylguanine in children and adolescents with refractory solid tumors. *Cancer Chemother Pharmacol* **65**:137–142.
9. **Patel M, McCully C, Godwin K, Balis FM.** 2003. Plasma and cerebrospinal fluid pharmacokinetics of intravenous temozolomide in nonhuman primates. *J Neurooncol* **61**:203–207.
10. **Rosset A, Spadola L, Ratib O.** 2004. OsiriX: An open-source software for navigating in multidimensional DICOM images. *J Digit Imaging* **17**:205–216.
11. **Saleem KS, Logothetis NK.** 2012. A combined MRI and histology atlas of the rhesus monkey brain in stereotaxic coordinates, 2nd ed. San Diego (CA): Academic Press.
12. **Scheller D, Kolb J.** 1991. The internal reference technique in microdialysis: a practical approach to monitoring dialysis efficiency and to calculating tissue concentration from dialysate samples. *J Neurosci Methods* **40**:31–38.
13. **Wang Y, Wong SL, Sawchuk RJ.** 1993. Microdialysis calibration using retrodialysis and zero-net-flux: application to a study of the distribution of zidovudine to rabbit cerebrospinal fluid and thalamus. *Pharm Res* **10**:1411–1419.